Glutathione-Mediated Metabolism of Technetium-99m SNS/S Mixed Ligand Complexes: A Proposed Mechanism of Brain Retention

Berthold A. Nock, Theodosia Maina, Drakoulis Yannoukakos, Ioannis C. Pirmettis, Minas S. Papadopoulos, and Efstratios Chiotellis*

Institute of Radioisotopes - Radiodiagnostic Products, NCSR "Demokritos", P.O. Box 60228, 153 10 Aghia Paraskevi, Athens, Greece

Received March 20, 1998

Two series of [^{99m}Tc](SNS/S) mixed ligand complexes each carrying the *N*-diethylaminoethyl or the *N*-ethyl-substituted bis(2-mercaptoethyl)amine ligand (SNS) are produced at tracer level using tin chloride as reductant and glucoheptonate as transfer ligand. The identity of [^{99m}Tc]-(SNS/S) complexes is established by high-performance liquid chromatographic (HPLC) comparison with authentic rhenium samples. The para substituent R on the phenylthiolate coligand (S) ranges from electron-donating ($-NH_2$) to electron-withdrawing ($-NO_2$) groups, to study complex stability against nucleophiles as a result of N- and R-substitution. The relative resistance of [^{99m}Tc](SNS/S) complexes against nucleophilic attack of glutathione (GSH), a native nucleophilic thiol of 2 mM intracerebral concentration, is investigated in vitro by HPLC. The reaction of [^{99m}Tc](SNS/S) complexes with GSH is reversible and advances via substitution of the monothiolate ligand by GS^- and concomitant formation of the hydrophilic [^{99m}Tc](SNS/GS) daughter compound. The *N*-diethylaminoethyl complexes are found to be more reactive against GSH as compared to the *N*-ethyl ones. Complex reactivity as a result of R-substitution follows the sequence $-NO_2 \gg -H > -NH_2$. These in vitro findings correlate well with in vivo distribution data in mice. Thus, brain retention parallels complex susceptibility to GSH attack. Furthermore, isolation of the hydrophilic [^{99m}Tc](SNS/GS) metabolite from biological fluids and brain homogenates provides additional evidence that the brain retention mechanism of [^{99m}Tc]-(SNS/S) complexes is GSH-mediated.

Introduction

Quantification of regional cerebral blood flow (rCBF) plays an important role in the diagnosis of various cerebrovascular and neurological disorders, among which are stroke, dementia, epilepsy, and psychiatric diseases.[1] The introduction of the ^{99m}Tc complex of hexamethylpropylene amine oxime (HM-PAO) in the late 1980s provided the first ^{99m}Tc-based radiopharmaceutical that can be successfully used in the clinic for the assessment of brain perfusion.[2] Originally, the use of [^{99m}Tc]HM-PAO was limited to only 30 min after labeling due to formation of radiochemical impurities soon after reconstitution of the commercial kit. This problem, which meanwhile has been efficiently addressed, prevented the preparation of [^{99m}Tc]HM-PAO in a central radiopharmacy unit and complicated its use in certain clinical investigations, as, for example, the imaging of epilepsy during the ictal phase.[3] To overcome these handicaps, the [^{99m}Tc]ethylcysteinate dimer (ECD) was later proposed due to its high chemical stability as a ^{99m}Tc brain perfusion imaging agent.[4] Both [^{99m}Tc]-HM-PAO and [^{99m}Tc]ECD are neutral lipophilic $^{99m}Tc^{V}O$ species that can cross the intact blood−brain barrier (BBB) by passive diffusion. They are then retained through different mechanisms in brain tissue for time sufficient to conduct single-photon emission-computed tomographic (SPECT) imaging using conventional instrumentation. Thus, whereas [^{99m}Tc]HM-PAO suffers nucleophilic attack by intracerebral glutathione (GSH) and transformation to hydrophilic species eventually decomposing to reduced hydrolyzed technetium,[5] [^{99m}Tc]-ECD is metabolized in brain cells to the corresponding free acid form after hydrolysis of at least one of its pendant ester groups by brain esterases.[4a,b,6] Given that [^{99m}Tc]ECD does not always accurately reflect rCBF in extreme conditions of low and high brain blood flow,[7] the search for the ideal ^{99m}Tc-based brain agent still continues.

Neutral, lipophilic ^{99m}Tc complexes can be alternatively generated following a different approach by coordination of a dianionic aminedithiolate and a monothiolate ligand to oxotechnetium.[8,9] In fact, the so-called "3 + 1" mixed ligand system primarily composed of the SNS/S donor atom combination has been the focus of our recent work.[9] Chemical studies with macroscopic amounts of ^{99g}Tc (carrier technetium) and rhenium have led to the complete characterization of this class of compounds. Comparison with the ^{99m}Tc (technetium tracer) analogues has demonstrated the formation of isostructural species, where the oxometal MO^{3+} core forms a neutral complex after binding the two ligands. The N-substituent of the tridentate ligand can adopt either a syn or an anti orientation with respect to the oxometal core, and thus, two isomers (syn and anti) are theoretically expected.[9] In most cases the major product is the syn isomer, with the anti isomer forming, if at all, in only negligible amounts.[9] The syn isomers adopt the unusual distorted trigonal-bipyramidal geometry

* To whom correspondence should be addressed. Tel: +301 6513 793. Fax: + 301 6543 526. E-mail: mainathe@mail.demokritos.gr.

10.1021/jm980174f CCC: $18.00
Published on Web 03/05/1999

Scheme 1. Preparation of [^{99m}Tc]- and Re(SNS/S) Mixed Ligand Complexes

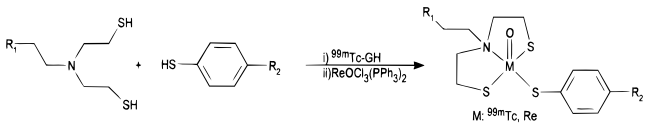

[^{99m}Tc](SNS/S) complex	Re(SNS/S) complex	R_1	R_2
1	**1′**	$N(CH_2CH_3)_2$	NH_2
2	**2′**	$N(CH_2CH_3)_2$	H
3	**3′**	$N(CH_2CH_3)_2$	NO_2
4	**4′**	H	NH_2
5	**5′**	H	H
6	**6′**	H	NO_2

around oxotechnetium, while the anti isomers prefer the familiar distorted square-pyramidal configuration.[9]

In a previous work we reported on the synthesis at tracer level and structure−activity relationships of a great number of [^{99m}Tc](SNS/S) complexes. In particular, the effect of the N-substituent on the tridentate ligand, as well as the type of monothiolate ligand on brain uptake and retention, has been studied. However, the mechanism responsible for the prolonged brain retention observed for many members of this series has not been established.[9f] Further findings later on concerning the stability of this system in the presence of excess thiol prompted us to study their stability versus nucleophilic attack of common native nonprotein thiols, like cysteine and GSH.[10] In particular, the γ-Glu-Cys-Gly tripeptide, involved in detoxification pathways of many xenobiotics, drew our attention due, on the one hand, to its highly nucleophilic thiolate group and, on the other hand, to its presence in 2 mM concentrations in brain cells.[11] Thus, a GSH-mediated retention mechanism for [^{99m}Tc](SNS/S) complexes was first postulated.

To test this hypothesis, we report herein on the in vitro stability versus GSH of two series of [^{99m}Tc](SNS/S) complexes each containing the *N*-diethylaminoethyl or the *N*-ethyl tridentate SNS ligand. Factors governing complex resistance to GSH are studied also in relation to monodentate ligand type. For this purpose, the stability versus GSH of complexes carrying either electron-donating ($-NH_2$) or electron-withdrawing ($-NO_2$) groups as the *p*-phenylthiolate substituent is compared. The in vitro findings of this study are then correlated with mice tissue distribution data with emphasis given on brain retention. Eventually, isolation of GSH-related metabolites from biological fluids, such as blood, bile, and urine, as well as from brain homogenates is also pursued, to provide additional evidence for the validity of our initial hypothesis.

Results and Discussion

Synthesis and Analysis of [^{99m}Tc](SNS/S) Complexes (Tracer Level). The [^{99m}Tc](SNS/S) mixed ligand complexes **1**−**6** are produced by ligand-exchange reaction using the [^{99m}Tc^{V}]glucoheptonate ([^{99m}Tc^{V}]GH) precursor, as described in Scheme 1. Due to the high affinity of the SNS/S donor atom set for technetium, the reaction is fast and practically quantitative (>90%), as determined by reverse-phase HPLC. Corroboration of structure with well-characterized analogous Re(SNS/S) complexes prepared (Scheme 1) at macroscopic amounts (**1**−**6′**)[9d−h] is achieved by HPLC, adopting both optical and γ detection modes. The identical chromatographic profiles summarized in Table 1 indicate formation of isostructural ^{99m}Tc and Re metal species.[9d−h] The complexes adopt a trigonal-bipyramidal geometry around the metal with the two sulfur atoms of the tridentate ligand and the oxygen atom defining the basal plane and the nitrogen atom of the tridentate ligand and the sulfur atom of the monothiol positioned each at the apexes of the distorted bipyramid.[9d−h] Although the N-substituent of the tridentate ligand has the possibility to be either syn or anti orientated with respect to the Tc═O core, the complexation reaction leads exclusively to the syn isomer.[9d−h]

Table 1. Retention Times of Technetium-99m and Rhenium SNS/S Complexes on a RP-HPLC Column[a]

[^{99m}Tc](SNS/S) complex	t_R (min)	Re(SNS/S) complex	t_R (min)
1	28.1	**1′**	27.9
2	29.7	**2′**	29.4
3	30.7	**3′**	30.5
4	26.1	**4′**	25.9
5	27.5	**5′**	27.3
6	29.0	**6′**	28.7

[a] For chromatograpic conditions, see text.

Scheme 2. Reversible Nucleophilic Attack of GSH on the Metal Center of [^{99m}Tc]- and Re(SNS/S) Mixed Ligand Complexes, Substitution of the Monothiolate Ligand, and Formation of the Respective Hydrophilic (SNS/GS) Metal Compound

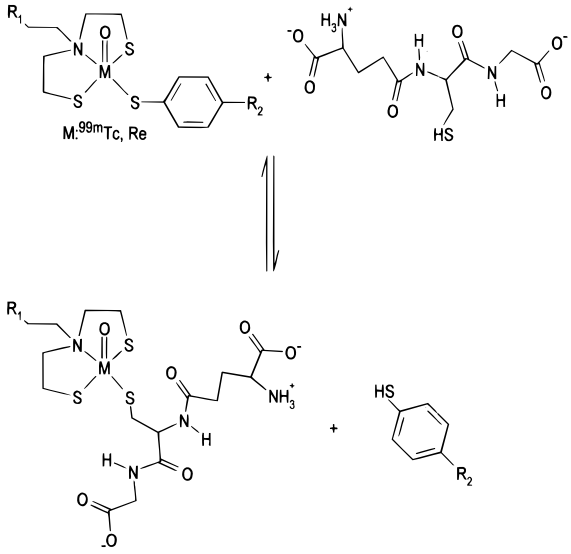

R_1	[^{99m}Tc](SNS/GS) complex	Re(SNS/GS) complex
$N(CH_2CH_3)_2$	**7**	**7′**
H	**8**	**8′**

In Vitro Reaction of [^{99m}Tc](SNS/S) Complexes with GSH. The interaction of [^{99m}Tc](SNS/S) mixed ligand complexes **1**−**6** with GSH in a phosphate-buffered solution of pH 7.4 at 37 °C is investigated. In all cases, as shown in Scheme 2, formation of a technetium daughter compound of hydrophilic character is revealed by HPLC analysis. The retention time (t_R) of this GSH-induced γ peak is identical for technetium complexes with the same tridentate ligand but differs slightly for the two series of technetium mixed ligand complexes under investigation. Thus, whereas the *N*-

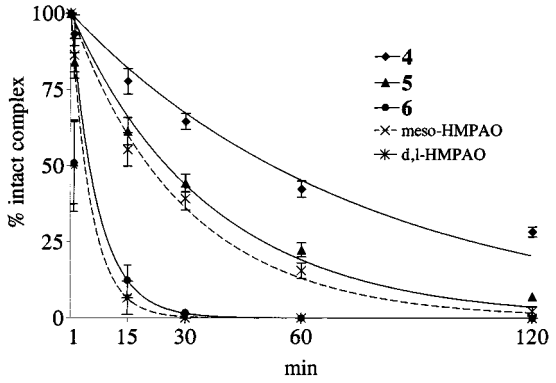

Figure 1. Rate of GSH-induced transformation of *N*-ethyl [^{99m}Tc](SNS/S) complexes to complex **8**. The GSH-induced decomposition of *d,l*-[^{99m}Tc]HM-PAO and *meso*-[^{99m}Tc]HM-PAO as a function of time is included for comparison. All data sets have been taken into account for the analysis presented in Table 2.

diethylaminoethyl [^{99m}Tc](SNS/S) complexes (**1**−**3**) after exposure to GSH transform to the daughter compound **7** of t_R 18.8 min, the *N*-ethyl ones (**4**−**6**) lead to the daughter hydrophilic species **8** of t_R 17.9 min under the applied chromatographic conditions.

The transformation rate not only depends on GSH concentration but is also strongly influenced by the type of tri- and monodentate ligands. In general, the members of the *N*-diethylaminoethyl series (**1**−**3**) react with GSH at a much faster pace than the members of the *N*-ethyl series (**4**−**6**). Concerning the monodentate ligands the transformation rate follows, for both series, the trend $-NO_2 \gg -H > -NH_2$. At a GSH concentration of 1 mM the time course of transformation of the *N*-ethyl series to **8** is summarized in Figure 1. The rate constants (k) and respective half-lives ($t_{1/2}$) for complexes **4**−**6** as well as those of the reference compounds ([^{99m}Tc]-*d,l*-HM-PAO and [^{99m}Tc]-*meso*-HM-PAO) are summarized in Table 2. Kinetic data for complexes **1**−**3** is not included, given that none of these compounds survives incubation with 1 mM GSH longer than 5 min. For the rate constants and respective half-lives for the interaction of GSH with **4**, **5**, and [^{99m}Tc]-*meso*-HM-PAO, the pseudo-first-order approach gives good results (see Figure 1). For complex **6** and [^{99m}Tc]-*d,l*-HM-PAO, the large uncertainty of the data point at 1 min is affecting the results for k; therefore, analyses have been carried out with and without this data point.

The GSH-induced transformation is shown to be reversible (Scheme 2). When purified complex **7** is reincubated with excess *p*-nitrothiophenol in phosphate buffer, the original mixed ligand complex **3** re-forms completely, as revealed by HPLC analysis.

Reaction of Re(SNS/S) with GSH ("carrier" level). Formation of the analogous rhenium complex **7′** is achieved after reacting complex **3′** with excess GSH in aqueous dimethylformamide. Chemical characterization of this compound verifies the formation of the *syn*-Re(SNS/GS) complex, which adopts a trigonal-bipyramidal geometry around the metal. Corroboration of structure with the ^{99m}Tc analogue **7** is performed by HPLC and is reported elsewhere in detail.[10d]

Similarly, after 1-h incubation of the rhenium analogue of **6′** with GSH at ambient temperature, HPLC analysis (UV detection at $\lambda = 382$ nm) demonstrates the formation of a hydrophilic daughter peak, complex **8′**, having the same t_R as the analogous daughter complex **8** formed after treatment of **6** with GSH. On the other hand, direct reaction of $CH_3CH_2N(CH_2CH_2SH)_2$ ligand and a 10-fold molar excess of GSH on the $Re^{V}OCl_3(PPh_3)_2$ precursor in aqueous DMF medium similarly leads to the formation of the daughter compound **8′**, as revealed by HPLC. When an equimolar quantity of GSH and ligand is applied, the reaction favors formation of a binuclear Re complex as already reported.[12]

In Vitro Reaction of [^{99m}Tc](SNS/S) Complexes with Cysteine. In contrast to their reversible reaction with GSH, where a defined γ peak is produced, the interaction of [^{99m}Tc](SNS/S) mixed ligand complexes **1**−**6** with cysteine leads irreversibly to short-lived unidentified daughter compounds, which decompose very rapidly to reduced hydrolyzed technetium.[10c] The latter reoxidizes over time to free [^{99m}Tc]pertechnetate in the open reaction vial. During HPLC and RP-18 TLC analyses of cysteine incubates, the major part (>80%) of the radioactivity remains on the column or at the origin of the TLC plates, respectively. The rate of cysteine attack is slightly increased compared to that of GSH for the same thiolate concentration.

In Vitro Reaction of *d,l*-[^{99m}Tc]HM-PAO and *meso*-[^{99m}Tc]HM-PAO with GSH. Given that the [^{99m}Tc](SNS/S) mixed ligand complexes transformation rate is crucial for brain retention, the decomposition rate of *meso*- and *d,l*-[^{99m}Tc]HM-PAO after GSH attack is performed under identical conditions and used as a reference (Figure 1). In contrast to the reaction of [^{99m}Tc](SNS/S) complexes with GSH, the incubation of *meso*- and *d,l*-[^{99m}Tc]HM-PAO with GSH leads to several decomposition peaks as well as reduced hydrolyzed technetium, as previously reported.[5] The decomposition rate of *meso*-[^{99m}Tc]HM-PAO is comparable to that observed for complexes **4** and **5** of the *N*-ethyl series after GSH incubation (Figure 1). However, in contrast to the *N*-ethyl [^{99m}Tc](SNS/S) complexes, which are stable in the absence of GSH and cysteine, the degradation of *meso*-[^{99m}Tc]HM-PAO is a result of both an "autodecomposition" (catalyzed by several factors, e.g., reductant, pH, buffer type) and an interaction with GSH.[3a,5d−f] On the other hand, the transformation rate of *d,l*-[^{99m}Tc]HM-PAO is faster than that of its *meso*-isomer[5a,b,c,f] and comparable to that found for the *N*-ethyl [^{99m}Tc](SNS/S) complex **6**. Both a more rapidly occurring "autodecomposition" and an enhanced susceptibility against GSH attack cause the observed increased decomposition rate of the *d,l*-[^{99m}Tc]HM-PAO isomer.[5a,c,f]

To interpret the above findings, the following mechanism is proposed. The [^{99m}Tc](SNS/S) complexes undergo nucleophilic attack on the metal center by the thiolate group of GSH leading to substitution of the monothiolate ligand by GS^-, as illustrated in Scheme 2. This assumption is strongly supported by the fact that the parent complexes are again regenerated from the corresponding daughter compounds (**7** or **8**) by reaction of excess of the respective monothiols. In this way, differences between complexes of the *N*-diethylaminoethyl and *N*-ethyl series can be reasonably explained. Thus, since each series contains another tridentate ligand, GSH attack leads to a distinct hydrophilic

Table 2. Pseudo-First-Order Rate Constants (k) and Corresponding Half-Lives ($t_{1/2}$) for the Interaction of Glutathione with **4**−**6** and the ^{99m}Tc Complexes of *meso*- and *d,l*-HMPAO

	4	**5**	**6**	*meso*-HMPAO	*d,l*-HMPAO
k (min^{-1})[a]	0.013 ± 0.0007	0.028 ± 0.002	0.13 ± 0.0075* 0.67 ± 0.088§	0.034 ± 0.002	0.18 ± 0.009* 0.69 ± 0.079§
$t_{1/2}$ (min)[b]	59 to 47	30 to 22	5.9 to 4.6* 1.4 to 0.8§	24 to 18	4.3 to 3.4* 1.3 to 0.8§

[a] The error bars have been calculated from measurements that have been repeated in triplicate. [b] 95% confidence intervals. With*/ without§ the 1-min time point.

daughter compound containing the original tridentate ligand (**7** from parent complexes **1**−**3** and **8** from parent complexes **4**−**6**). The same holds true for the analogous Re complexes **7′** and **8′** formed in macroscopic amounts after treatment of complexes **3′** and **6′**, respectively, with excess GSH in aqueous dimethylformamide medium. The isolation and chemical characterization of complex **7′**, reported elsewhere,[10d] provides further evidence to support the above hypothesis. In addition, daughter compound **8′** is also prepared in good yield by direct reaction of the *N*-ethyl tridentate ligand and GSH on the $Re^{V}OCl_3(PPh_3)_2$ precursor in a 1:10:1 molar ratio. Analysis by HPLC demonstrates the structural analogy between the Re and ^{99m}Tc metal species.

The trend observed in the conversion rate for both series ($-NO_2 \gg -H > -NH_2$) can be attributed to electronic effects imposed by the para substituent of the phenylthiolate ligand.[10c] It is the electron-withdrawing character of the $-NO_2$ group that favors the attack of nucleophiles, whereas the electron-donating quality of the $-NH_2$ group exerts the opposite effect. On the other hand, the pronounced difference in the conversion rate between the *N*-diethylaminoethyl and *N*-ethyl series is more subtle to interpret, given that the immediate metal coordination sphere is the same for both series of complexes. In the syn configuration of the *N*-diethylaminoethyl M(SNS/S) complexes, the tertiary pendant amine group, which is protonated under physiological conditions, can come in close vicinity to the electron-rich oxygen atom of the oxometal core. This electrostatic interaction may induce a reduced electron density on the metal atom, thereby "intramolecularly catalyzing" the nucleophilic attack of GSH (Scheme 3, A). In an alternative approach, the GSH substitution reaction on the parent *N*-diethylaminoethyl ^{99m}Tc(SNS/S) complexes is facilitated by an intramolecular proton transfer from the protonated pendant amine to the departing phenylthiolate (Scheme 3, B).[14b−e]

In contrast, the reaction of [^{99m}Tc](SNS/S) complexes with cysteine causes their decomposition to reduced hydrolyzed technetium.[10c] The decomposition rate parallels their GSH-mediated transformation rate, although it proceeds at a slightly faster pace. This can be well-explained both by the lower pK_a value of cysteine (8.38 for cysteine versus 8.97 for GSH)[13] and by mobility factors, given that cysteine is a smaller molecule in comparison to the tripeptide.[5e] In the case of [^{99m}Tc]HMPAO both cysteine and GSH provoke the decomposition of the metal complex, but the mechanism of this reaction is still unclear.[5] The discrepancy between cysteine and GSH effect, observed for the [^{99m}Tc](SNS/S) complexes, may be assigned to the electronic influence of either the free amine or the free carboxylate group of cysteine. Assuming that a short-lived intermediate [^{99m}Tc](SNS/Cys) complex forms after cysteine attack, these functional groups may act by anchimeric assistance as intramolecular nucleophiles on the β-carbon atom of S-coordinated cysteine.[14a] As a result, the reactive nucleofugal [^{99m}Tc](SNS/S$^-$) species is released, which eventually decomposes to reduced hydrolyzed technetium, as depicted in Scheme 4. The above neighboring-group mechanism is currently under investigation, with the goal to demonstrate the formation of the labile [^{99m}Tc](SNS/S$^-$) anion.

Scheme 3. Two Possible Mechanisms for Explaining the Increased Reactivity of the *N*-Diethylaminoethyl Complexes against GSH[a]

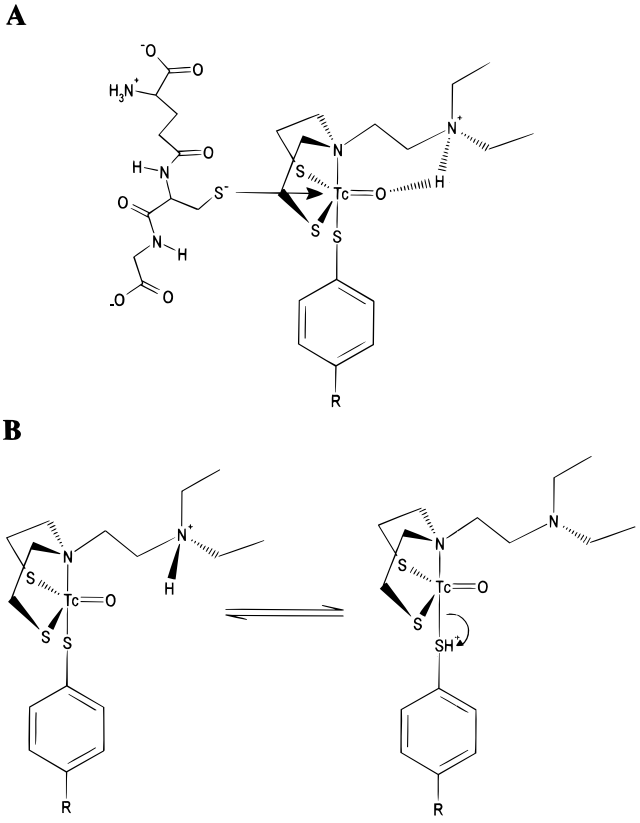

[a] A: Nucleophilic attack of glutathione on the technetium metal center of *syn*-[^{99m}Tc](SNS/S) mixed ligand complexes facilitated by an additionally induced positive charge through the intramolecular hydrogen bridge between the oxygen of the TcO core and the protonated pendant amine. B: "Tautomeric" transition state, in which the proton moves from the pendant amine to the leaving phenylthiolate facilitating its departure.

Analysis of Complex 3 Incubates in Mouse Blood. The distribution of radioactivity between serum and red blood cells (RBCs) after incubation of **3** in mouse blood at 37 °C is found to be different at 1- and 45-min incubation periods. Whereas at 1-min incubation RBCs contain 60% of total radioactivity with the remaining activity found in serum, at 45 min only 20% of total radioactivity is still retained in RBCs. When the RBCs

Scheme 4. Irreversible Nucleophilic Attack of Cysteine on [^{99m}Tc](SNS/S) Mixed Ligand Complexes Leading, in the Absence of Electrophiles, to Reduced Hydrolyzed ^{99m}Tc

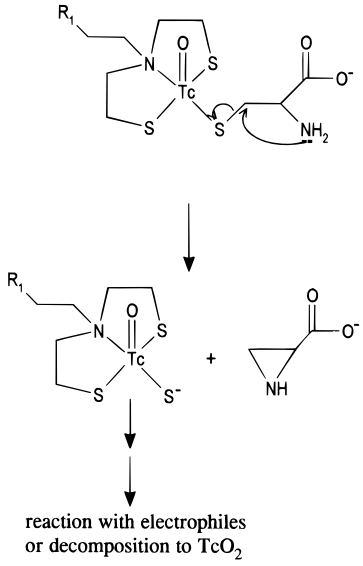

membranes are broken the radioactivity is found exclusively in the cytosol. Analysis by HPLC of mouse plasma after 1-min incubation of **3** in total mouse blood demonstrates an 80% presence of the original complex **3** together with 20% of only one hydrophilic metabolite. However, at 45 min all plasma **3** is completely transformed to the same hydrophilic compound, identified as the daughter compound **7**. It seems that complex **3** enters the RBCs by passive diffusion, wherein it suffers nucleophilic attack by GSH (RBCs GSH concentration 2 mM)[11] and transforms to **7**. The latter is actively transported into plasma with time by a GS-X conjugate-related transporter protein,[11,15] since its hydrophilic character prevents its passive rediffusion into serum through the RBCs membrane. In fact, analysis by HPLC of the cytosol fractions of mouse RBCs reveals the complete transformation of **3** already after 1-min incubation to **7**. In this case, an additional and slightly more hydrophilic peak (t_R: 16.8 min) is also detected. It can be postulated that this secondary peak is a further metabolic product of complex **7**.[16]

Analysis of Complex 3 Incubates in Mouse Brain Homogenates. As revealed by HPLC analysis of complex **3** 1-min incubates in mouse brain homogenates, 80% of radioactivity is found in the solute, whereas 20% is found bound to proteins. The non-protein-bound activity is identified as the hydrophilic daughter complex **7**. At 45 min the percentage of protein-bound activity increases to 50%, while the remaining 50% is again conclusively assigned to complex **7**. Formation of further metabolites of complex **7** (dipeptide, cysteine, and *N*-acetylcysteine), reported for other GS-X conjugates,[16] is totally absent from the solute. However, their formation cannot be ruled out, if the increase in protein-binding metabolites with time on the one hand and the high instability of the respective [^{99m}Tc](SNS/cysteine) complex on the other hand are taken into account.

Subcellular Distribution of Complex 3 in Mouse Brain. The major part of radioactivity (>80%) in mouse brain cells after administration of complex **3** is found in the mitochondrial and cytosol fractions, as shown by fractional centrifugation. The remaining radioactivity (20%) is equally divided between the nuclear and microsomal membrane fractions.[17] This distribution does not significantly differ between the 1- and 45-min preparations. Analysis by HPLC of the cytosol fraction demonstrates the existence of only the hydrophilic metabolite **7**.

Isolation of Complex 3 Metabolites in Mice. a. Metabolites in bile: Analysis by HPLC of mouse bile after administration of complex **3** demonstrates its total absence in the bile. Instead, metabolite **7** together with a slightly more hydrophilic derivative of t_R: 16.9 min are present in a 55/45 ratio.

b. Metabolites in the Urine: Similarly, HPLC analysis of mouse urine reveals the total absence of the original complex **3**. The predominant metabolite found by 60% in the urine coelutes at a t_R of 18.8 min with the daughter GSH-induced complex **7**.

Biodistribution of [^{99m}Tc](SNS/S) Complexes in Mice. The tissue distribution of radioactivity after intravenous (iv) administration of [^{99m}Tc](SNS/S) mixed ligand complexes in mice is performed, and blood and brain clearance data are shown in Figure 2. It is generally observed that all complexes exhibit a fast blood clearance. Significant accumulation of radioactivity is found in liver, lung, and kidneys—organs known for their high intracellular GSH content.[11] The radioactivity is cleared out not only through the liver and intestines but also via the kidneys and the urinary tract. Analysis of mouse bile after iv administration of complex **3** reveals the presence of two hydrophilic metabolites. One is clearly identified as the GS^--containing daughter compound **7**, whereas the second one is attributed to further metabolism of **7** in the liver.[11,16,18a] At longer time intervals a substantial portion of the radioactivity is found in the urine. In this case also, HPLC analysis of the urine reveals a series of hydrophilic metabolites, among which daughter complex **7** is the major product (60%).

Retention data in mouse brain for the *N*-diethylaminoethyl and the *N*-ethyl series is presented as brain/blood ratio values in Figure 2 as a function of time. Brain retention is observed only for the members of the *N*-diethylaminoethyl series, as expected from the in vitro data described above. Since these complexes react rapidly with GSH and transform fast to the hydrophilic metabolite **7**, they are consequently trapped into brain cells. In fact, the daughter technetium complex **7** cannot recross the BBB by passive diffusion, as a result of its hydrophilic character. This fact is confirmed by the biodistribution of **7** in mice, revealing the negligible brain uptake of this compound (0.01% ID/g at 1 min pi). However, the brain retention observed for the *N*-diethylaminoethyl complexes is not as long lasting as that of [^{99m}Tc]HM-PAO. The latter irreversibly decomposes to reduced hydrolyzed ^{99m}Tc in brain cells.[2,3,5] Transport proteins on the cell membrane, known to actively translocate GS-X conjugates out of the cell, are suspected for the eventual washout of the *N*-diethylaminoethyl complex metabolite from the brain.[15,19] This holds true also for the observed declining retention of complex **3** in RBC.[15] In contrast, the *N*-ethyl series complexes react with GSH at a substantially slower

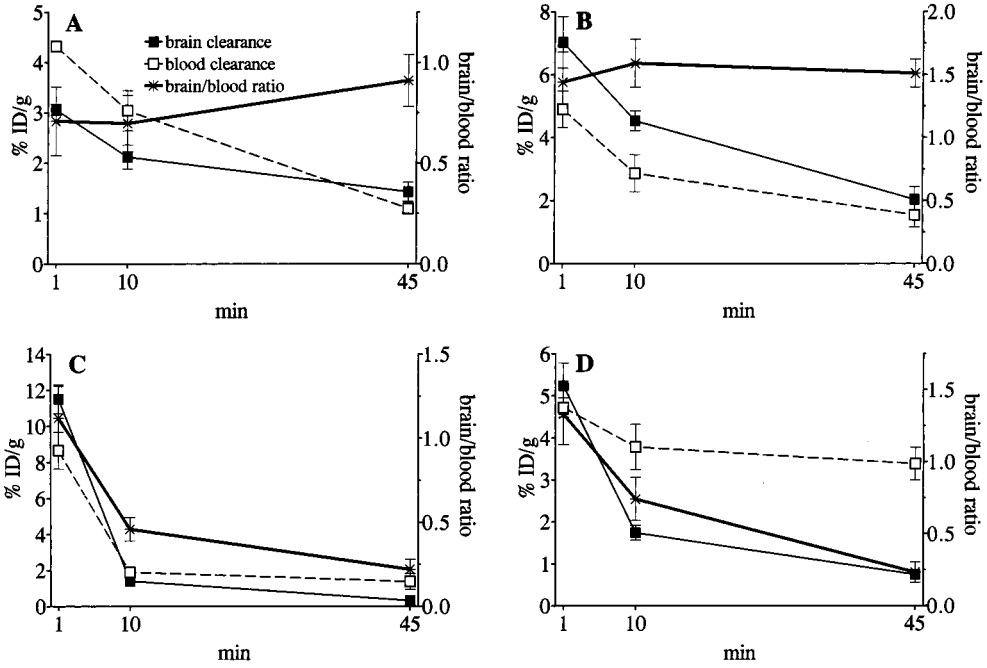

Figure 2. Brain-to-blood ratios over time after iv administration of [^{99m}Tc](SNS/S) complexes **1**, **3**, **4**, and **6** in mice.

rate, not sufficiently fast to prevent their passive diffusion through the BBB back into the blood stream. As a consequence, they wash out of brain cells over time without being sufficiently retained (Figure 2). It is evident that the in vitro findings correlate well with in vivo data, thereby strongly supporting the assumption that the brain retention of [^{99m}Tc](SNS/S) mixed ligand complexes is GSH-mediated.

Conclusions

The above-described study has elucidated the brain retention mechanism of [^{99m}Tc](SNS/S) mixed ligand complexes. This mechanism involves the rapid nucleophilic attack of intracerebral GSH on the complex metal center, substitution of the monothiolate ligand by GS^-, and formation of the hydrophilic [^{99m}Tc](SNS/SG) metabolite. It is reported that human intracerebral GSH concentration ranges from approximately 2.2 mM for healthy brain to 0.8 mM for diseased brain, as revealed by studies of autopsied or biopsied brain.[5d,11,20a−c] Brain disorders involving changes of intracerebral GSH content include Alzheimer's and Parkinson's diseases, as well as brain injury induced by ischemia, inflammation, or aging.[5,11,20] Therefore, a ^{99m}Tc agent able to in vivo assess intracerebral GSH levels is of particular importance. For this purpose, *meso*-[^{99m}Tc]HM-PAO has been proposed by certain research groups as an imaging agent for the GSH localization in the brain of humans.[5d−f] However, the [^{99m}Tc](SNS/S) mixed ligand complexes may be applied more successfully for the same purpose, given that their brain trapping mechanism is directly GSH concentration-dependent and is not a combined effect of a parallel "autodecomposition" process, as in the case of *meso*-[^{99m}Tc]HM-PAO.[5d−f] Moreover, since the rate of GSH-induced transformation of such an agent must be sensitive to alterations in GSH levels, this system offers the additional possibility of "fine-tuning" complex susceptibility toward the desired GSH "concentration-window" by careful selection of the tri- and/or monodentate ligand.

An additional option of this system concerns ^{99m}Tc diagnosis in oncology. Recent studies have demonstrated that elevated tumor GSH intracellular levels are often detected after cytoreductive chemotherapy, leading to tumor cell resistance to the applied therapeutic scheme.[21] Thus, selected [^{99m}Tc](SNS/S) mixed ligand complexes may turn out to provide a valuable prognostic tool for the efficacy of cytostatic chemotherapy interfering with tumor intracellular GSH levels.

Eventually, the usefulness of [^{99m}Tc](SNS/S) mixed ligand complexes for carrying a pharmacophore group to particular brain receptors[22] can be evaluated after their resistance against GSH attack is first established. However, the introduction of the pharmacophore group on the tridentate ligand may, after GSH attack, lead to a prolonged residence of the hydrophilic [^{99m}Tc](SNS/SG) metabolite still carrying the pharmacophore group in the immediate vicinity of the respective receptor sites in brain tissue, thereby enhancing the probability of receptor−ligand interactions without necessarily negatively affecting the receptor affinity of the forming radioligand at the same time.

In conclusion, the elucidation of brain retention mechanism of [^{99m}Tc](SNS/S) mixed ligand complexes has revealed the potential of the SNS/S mixed ligand system in the diagnosis of several pathologies interfering with intracellular GSH levels.

Experimental Section

Safety Note! Technetium-99m (^{99m}Tc) is a γ emitter (141 keV) with a half-life of 6 h. Work with solutions containing this radionuclide must always be performed behind sufficient lead shielding.

General. All chemicals were of reagent grade unless noted otherwise. *p*-Nitrothiophenol, thiophenol, and *p*-aminothiophenol were purchased from Fluka. Synthesis and purification of $CH_3CH_2N(CH_2CH_2SH)_2$ and $(CH_3CH_2)_2NCH_2CH_2N(CH_2CH_2SH)_2$ were performed according to reported protocols.[23] Technetium-99m was used as a [^{99m}Tc]$NaTcO_4$ solution in physiological saline either as an in-house preparation (Techne/Demoscan, NCSR "Demokritos") or as a commercial ^{99}Mo/^{99m}Tc

generator eluate (Cis International). The [^{99m}Tc]Tc^{V}-glucoheptonate ([^{99m}Tc]Tc^{V}-GH) was produced by reconstitution of commercial kits (Gluco/Demoscan, NCSR "Demokritos") that contain a lyophilized mixture of $SnCl_2$ (0.2 mg, 1.05 μmol) and glucoheptonate (200 mg, 0.408 mmol). Solvents for high-performance liquid chromatography (HPLC) were of HPLC grade; they were filtered through membrane filters (0.45 μm; Millipore, Milford) and degassed by helium flux before use.

HPLC analysis was conducted on a Waters 600 Millenium chromatography system coupled to both a Waters 486 tunable absorbance detector set either at 254 or 382 nm and a Steffi γ detector obtained from Raytest (RSM Analytische Instrumente GmbH, Germany). Separations were achieved on a Techsil 10CN column (10 μm, 4.6 mm × 250 mm) eluted with a binary gradient system at a flow rate of 1 mL/min. Mobile phase A consisted of a 2% aqueous solution of triethylamine neutralized to pH 7.1 with 85% phosphoric acid, while mobile phase B was pure ethanol. The elution profile was 0−3 min isocratic with mobile phase A, followed by a linear gradient to 30% A in 20 min; this composition was held for another 10 min. After a column wash with 95% B for 5 min, the column was reequilibrated with mobile phase A for 20 min prior to next injection.

Thin-layer chromatography (TLC) was performed on (A) reversed-phase Whatman KC18 plates developed with ethanol/HPLC mobile phase A [90/10], (B) Whatman no. 1 paper using acetonitrile/water, 50/50 (v/v), or (C) 0.25-mm Merck silica gel coated aluminum F_{254} plates, and (D) Whatman no. 1 paper strips developed with ether. The plates were scraped, and the radioactivity was counted in a Packard Auto Gamma 5000 Series γ counter (Chicago, IL).

Synthesis of [^{99m}Tc](SNS/S) Complexes (tracer level). A commercial kit (Gluco/Demoscan, NCSR "Demokritos") was reconstituted with water (10 mL), and an aliquot (1 mL) was withdrawn and mixed with [^{99m}Tc]pertechnetate solution (0.5−1.0 mL, 5−10 mCi). The resulting [^{99m}Tc^{V}]O-GH solution was added to a centrifuge tube containing equimolar amounts (0.02 mmol) of the tri- and monodentate ligand. The mixture was agitated on a vortex mixer for 1 min and left to react at room temperature for 10 min. The lipophilic [^{99m}Tc](SNS/S) complex was extracted into dichloromethane (3 × 2 mL) and the organic phase dried over $MgSO_4$, filtered, and reduced to a small volume (0.5−1 mL) under a gentle stream of nitrogen at 25 °C. Aliquots of this solution (100 μL, ≈ 1 mCi) were purified by HPLC by eluting a Waters μPorasil column (10 mm, 3.9 × 300 mm) with dichloromethane/methanol either in a 99/1 (*N*-ethyl complexes **4**−**6**) or in a 95/5 (*N*-diethylaminoethyl complexes **1**−**3**) v/v ratio as eluent at a flow rate of 1 mL/min. The fractions containing the [^{99m}Tc](SNS/S) complex alone were collected and evaporated to dryness under a mild nitrogen stream. The [^{99m}Tc](SNS/S) complex was redissolved in ethanol and for the biodistribution experiments further diluted with physiological saline to a final 20% ethanol/saline (v/v) solution containing the desired radioactivity.

Corroboration of [^{99m}Tc](SNS/S) Structure with the Analogous Re(SNS/S) Complexes. The synthesis and chemical characterization of the analogous Re(SNS/S) complexes **1′**−**6′** are reported elsewhere.[9e,g,h] Briefly, the complexes were synthesized by reacting equimolar amounts of tridentate and monodentate ligands on the Re$^{V}OCl_3(PPh_3)_2$ precursor in dichloromethane/methanol mixtures, as presented in Scheme 1. Purification of the products was achieved by repeated recrystallizations. Classical methods of analysis (elemental analysis, IR, UV/vis, ^{1}H and ^{13}C NMR spectroscopies, and X-ray structural analysis) are used for their characterization. By co-injection of prototype solutions of the Re complexes and their ^{99m}Tc analogues on the HPLC column using parallel UV/vis and γ detection, their chromatographic behavior was compared. Elutions were performed using the conditions described above.

In Vitro Reaction of [^{99m}Tc](SNS/S) Complexes with GSH. In a polypropylene test tube (1.5 mL) containing 0.2 M phosphate buffer (250 μL, pH 7.4) were added water (150, 195 μL) and HPLC-purified [^{99m}Tc](SNS/S) (50 μCi) dissolved in ethanol (50 μL). An aliquot (50, 5 μL) of a 10 mM stock solution of GSH in 10 mM HCl was added, and the mixture was incubated in a water bath at 37 °C. For the blank an equal volume of distilled water was added instead of GSH solution. All solutions were purged with nitrogen prior to use, and incubation was conducted in a sealed vial. Aliquots of the incubate (1 and 50 μL) withdrawn at 1-, 15-, 30-, and 60-min and 2-h time intervals were analyzed by TLC system A and HPLC, respectively. The column radioactivity recovery amounted to 90%. Column recovery was calculated by comparison of the γ activity of 1 mL of collected HPLC eluate with 1% of the injected activity dissolved in 1 mL of HPLC eluent.

Re-formation of Complex 3 from the Hydrophilic Daughter Compound 7. The HPLC-purified [^{99m}Tc]complex **6** (≈1 mCi) was incubated in GSH solution (1 mL of 0.01 mM GSH in 0.1 M phosphate buffer, pH 7.4) for 60 min at room temperature. An aliquot (25 μL) of this incubate was analyzed by HPLC to verify complete transformation of **6** to the more hydrophilic daughter ^{99m}Tc species **7**. Thereafter, the incubation mixture was loaded onto an activated OASIS extraction cartridge, the cartridge was rinsed with 5% methanol/saline (1 mL), and the radioactivity was eluted with methanol (1 mL). The methanol fraction was evaporated to dryness under a N_2 stream and slightly warmed at 40 °C in a water bath. The residue was redissolved in phosphate buffer (250 μL, 0.2 M, pH 7.4) and further diluted with water (200 μL). A suspension of *p*-nitrophenol in 50% ethanol/water (50 μL, 0.1 M) was added, and the mixture was left to react for 10 min at 37 °C. An aliquot (50 μL) thereof was withdrawn and subjected to HPLC analysis under the same chromatographic conditions as before.

Reaction of Re(SNS/S) with GSH ("carrier" level). To a green solution of **3′** (5.0 mg, 8.46 μmol) in dimethylformamide/dichloromethane (1/1 v/v, 5 mL) was added an aqueous solution of GSH (50 mg, 0.16 mmol in 1 mL). After 1 h of stirring at room temperature an aliquot (25 μL) of the resulting green reaction mixture containing the daughter compound **7′** was subjected to HPLC analysis with UV wavelength detection set at λ = 382 nm and using the same elution conditions as before.

The hydrophilic complex **8′** was similarly prepared by reacting excess GSH on complex **6′** in aqueous dimethylformamide medium. Alternatively, complex **8′** was also prepared by reacting the $CH_3CH_2N(CH_2CH_2SH)_2$ ligand (33 mg, 0.2 mmol) and a 10-fold molar excess of GSH (615 mg, 2 mmol) with Re$^{V}OCl_3(PPh_3)_2$ (166.6 mg, 0.2 mmol) in a dimethylformamide−water mixture (5 mL, 1/1 v/v). After short refluxing the reaction mixture turned green, whereupon it was diluted with water (5 mL) and washed with dichloromethane (3 × 5 mL). Aliquots (20 μL) of the aqueous phase were withdrawn and subjected to HPLC analysis under the same conditions as above.

In Vitro Reaction of [^{99m}Tc](SNS/S) Complexes with Cysteine. The procedure described above for the GSH challenge experiments was similarly followed, but instead of using GSH stock solution (10 mM) an aqueous solution of cysteine hydrochloride (10 mM) was employed.

In Vitro Reaction of *d,l*-[^{99m}Tc]HM-PAO and *meso*-[^{99m}Tc]HM-PAO with GSH. *d,l*-[^{99m}Tc]HM-PAO and *meso*-[^{99m}Tc]HM-PAO were prepared according to a reported protocol.[2,3,5] Briefly, [^{99m}Tc]pertechnetate (20−25 mCi, 5 mL) was added to a vial containing the respective ligand (1 mg). A freshly prepared solution (10 mL) of stannous chloride (10 mg in 10 mL of N_2-purged 0.1 M HCl) was used as reductant. The lipophilic technetium complexes were extracted in diethyl ether (2 mL), and the ether phase was evaporated to dryness under a N_2 stream. The residue was redissolved in ethanol (0.5 mL) and then diluted with physiological saline (2 mL). The radiochemical purity was tested by HPLC under the same conditions, as in the case of the [^{99m}Tc](SNS/S) complexes.

The GSH challenge experiments were performed at 1 mM GSH concentration as described above for the [^{99m}Tc](SNS/S) complexes. The percentage of intact lipophilic *d,l*-[^{99m}Tc]HM-PAO or *meso*-[^{99m}Tc]HM-PAO complex was determined by both HPLC and TLC system D.[3a]

Analysis of Complex 3 Incubates in Mouse Blood. Swiss Albino mice (35 ± 3 g) were anesthetized under ether and sacrificed by cardiac puncture. Mouse blood was immediately collected into heparin-treated syringes. Aliquots (1 mL) were incubated at 37 °C with HPLC-purified [^{99m}Tc](SNS/S) complex (500 μCi in 100 μL of 20% ethanol/saline v/v). Incubates of 1 and 45 min were centrifuged to separate plasma from red blood cells (RBCs). An aliquot (100 μL) of the plasma phase of each incubate was then diluted with physiological saline to 1 mL and further eluted through an OASIS extraction cartridge as described above. Aliquots (10 μL) of the OASIS eluate fractions were measured in the γ counter for their radioactivity content, and the methanol fraction was analyzed by HPLC using the same system. The RBCs were resuspended in a hypotonic lysis buffer (20 vol, 5 mM phosphate buffer, pH 7.8, 1 mM EDTA, 0.1 mM PMSF) for 5 min and centrifuged at 4 °C for 20 min at 10 000 rpm. Pellet and supernatant were counted for their radioactivity content, and the latter also was eluted through an OASIS extraction cartridge and analyzed by HPLC.

Analysis of Complex 3 Incubates in Mouse Brain Homogenates. Swiss albino mice (35 ± 3 g) were sacrificed by cardiac puncture under a slight ether anesthesia. Whole brain was immediately removed, put on ice, and homogenized in ice-cold phosphate-buffered sucrose (5 mL of 0.25 M sucrose, 0.01 M phosphate, pH 7.4) using a Jahnke & Kunkel homogenizer set at 1/2 max for 30 s. Aliquots of HPLC-purified [^{99m}Tc](SNS/S) (300 μCi in 100 μL of 20% ethanol/saline) were added to the brain homogenate (2 mL) and incubated at 37 °C. Aliquots (1 mL) of 1- and 45-min incubates were loaded onto an activated OASIS extraction cartridge, and the same procedure was followed as before.

Subcellular Distribution of Complex 3 in Mouse Brain. Mice were injected with HPLC-purified [^{99m}Tc](SNS/S) (80 μCi) through the tail vein under ether anesthesia. The animals were sacrificed at 1 and 45 min postinjection (pi) by cardiac puncture and the brains excised, placed on ice, and immediately homogenized as described above. The homogenates were subjected to fractional centrifugation following modified reported methods,[4a,b,24] in order to determine the distribution of the radioactivity in mouse brain cells. Briefly, by successive centrifugation: (i) 3× for 5 min at 650 g, (ii) 20000*g* for 15 min, and (iii) 100000*g* for 60 min the nuclear membrane, mitochondrial, microsomal and cytosol fractions were respectively collected. Pellets and final supernatant divided in smaller volume samples were measured for their radioactivity content in an automated γ counter. Values were corrected for radioactive decay by use of appropriate standard solutions. The cytosol fraction was subjected to the same process as described above for the RBC and eventually analyzed by HPLC using the same chromatographic conditions.

Isolation of Complex 3 Metabolites in Mice. a. Metabolites in bile: A bolus of HPLC-purified [^{99m}Tc](SNS/S) (80 μCi, 80−100 μL of 20% v/v ethanol) was injected in the tail vein of ether anesthetized mice. The animals were sacrificed 45 min pi and the gall bladders excised. The bile was collected, and aliquots (200 μL) were diluted with physiological saline to 1 mL. This mixture was applied onto an OASIS extraction cartridge already prewashed with methanol (1 mL) and activated with physiological saline (1 mL). After application of the sample, the same procedure was followed as before.

b. Metabolites in the urine: In a similar manner, the animal bladder was excised and the urine collected with a syringe. Cartridge purification and HPLC analysis were performed as above.

Biodistribution of [^{99m}Tc](SNS/S) Complexes in Mice. Biodistribution experiments were performed in groups of five male Swiss Albino mice (30−34 g). The mice were administered HPLC-purified [^{99m}Tc](SNS/S) (2−3 μCi in 100 μL of 20% v/v ethanol) through tail vein injection. The animals were sacrificed by cardiac puncture under a slight ether anesthesia at 1-, 10-, and 45-min time intervals. The organs of interest were excised, weighed, and counted for their radioactivity content in an automatic γ counter. The stomachs and intestines were not emptied of food contents prior to radioactivity measurements. The percentage of injected dose per organ (% ID/organ) was calculated by comparison to standard solutions containing 1% of the injected dose. The calculation for blood was based upon measured activity, sample weight, and body composition data (considering that blood comprises 7% of mouse body weight). The percentage of injected dose per gram (% ID/g) was calculated by dividing the respective % ID/organ by the weight of the organ or tissue. The brain/blood ratio was calculated by dividing the respective % ID/g values.

Biodistribution of the Hydrophilic Daughter Compound 7 in Mice. The biodistribution of the hydrophilic [^{99m}Tc](SNS/GS) complex was conducted as described above. The OASIS isolated technetium complex was redissolved in 20% ethanol/saline (v/v) to produce the desired activity concentration for injection.

Supporting Information Available: Representative chromatograms for the formation of GS-X analogues at tracer and carrier levels, as well as in biological fluids (Figures 1 and 2), and tissue distribution data as % ID/g for complexes **1**, **3**, **4**, **6**, and **7** in mice (Figures 3 and 4). This material is available free of charge via the Internet at http://pubs.acs.org.

References

(1) (a) McIntosh, T. K. Neurochemical sequela of traumatic brain injury: therapeutic implications. *Cerebrovasc. Brain Metab. Rev.* **1980**, *6*, 109−162. (b) Hill, T. C.; Holman, B. L. SPECT brain imaging: finding a niche in neurological diagnosis. *Diag. Imag.* **1985**, *7*, 64−68. (c) Holman, B. L.; Hill, T. C. Functional imaging of the brain with SPECT. *Appl. Radiol.* **1984**, *13*, 21−27. (d) Pickard, J. D.; Read, D. H.; Lovick, A. H. J. Use of cerebral blood flow measurements in the prediction of delayed cerebral ischemia following subarachnoid hemorrhage. *Cerebral blood flow and metabolism measurement*; Springer-Verlag: Berlin, Heidelberg, 1985; pp 149−152. (e) Bonte, F. J. SPECT study of brain blood flow in seizure disorders and psychiatric diseases. *Curr. Concepts in Diag. Nucl. Med.* **1987**, 9−15. (f) Ell, P. J.; Jarritt, P. H.; Costa, D. C.; Cullum, I. D.; Lui, D. Functional imaging of the brain. *Semin. Nucl. Med.* **1987**, *17*, 214−229.

(2) (a) Holmes, R. A.; Chaplin, S. B.; Royston, K. G.; et al. Cerebral uptake and retention of Tc-99m hexamethylpropylene amine oxime (Tc-99m HM-PAO). *Nucl. Med. Commun.* **1985**, *6*, 443−447. (b) Sharp, P. F.; Smith, F. W.; Gemmell, H. G.; et al. Technetium-99m HM-PAO stereoisomers as potential agents for imaging regional cerebral blood flow. *J. Nucl. Med.* **1986**, *27*, 171−177. (c) Nowotnik, D. P.; Canning, L. R.; Cumming, S. A.; et al. Tc-99m-HM-PAO: a new radiopharmaceutical for imaging regional cerebral blood flow. *J. Nucl. Med. Allied Sci.* **1985**, *29*, 208. (d) Neirinckx, R. D.; Canning, L. R.; Piper, I. M.; Nowotnik, D. P.; et al. Technetium-99m d, l-HM-PAO: A new radiopharmaceutical for SPECT imaging of regional cerebral blood perfusion. *J. Nucl. Med.* **1987**, *28*, 191−202.

(3) (a) Hung, J. C.; Corlija, M.; Volkert, W. A.; Holmes, R. A. Kinetic analysis of technetium-99m d,l-HM-PAO decomposition in aqueous media. *J. Nucl. Med.* **1988**, *29*, 1568−1576. (b) Newton, M. R.; Austin, M. C.; Chan, J. G.; McKay, W. J.; Rowe, C. C.; Berkovic, S. F. Ictal SPECT using technetium-99m-HMPAO: methods for rapid preparation and optimal deployment of tracer during spontaneous seizures. *J. Nucl. Med.* **1993**, *34*, 666−670.

(4) (a) Walovitch, R. C.; Makuch, J.; Garrity, S.; et al. Neuropharmacological characterization of Tc99m ECD in human and nonhuman primates. *Neurology* **1988**, *38*, 363. (b) Walovitch, R. C.; Hill, T. C.; Garrity, S. T.; Cheesman, E. H.; et al. Characterization of technetium-99m−L,L-ECD for brain perfusion imaging, Part 1: Pharmacology of technetium-99m ECD in nonhuman primates. *J. Nucl. Med.* **1989**, *30*, 1892−1901. (c) Leveille, J.; Demonceau, G.; DeRoo, M.; et al. Characterization of technetium-99m-L,L-ECD for brain perfusion imaging, Part 2: Biodistribution and brain imaging in humans. *J. Nucl. Med.* **1989**, *30*, 1902−1910. (d) Papazyan, J. P.; Delavelle, J.; Burkhard, P.; Rossier, P.; et al. Discrepancies between HMPAO and ECD SPECT imaging in brain tumors. *J. Nucl. Med.* **1997**, *38*, 592−596.

(5) (a) Neirinckx, R. D.; Burke, J. F.; Harrison, R. C.; Forster, A. M.; Andersen, A. R.; Lassen, N. A. The retention mechanism of technetium-99m-HM-PAO: Intracellular reaction with glutathione. *J. Cereb. Blood Flow Metab.* **1988**, *8*, S4−S12. (b) Suess, E.; Malessa, S.; Ungersboeck, K.; Kitz, P.; Podreka, I.; Heimberger, K.; Hornykiewicz, O.; Deecke, L. Technetium-99m-d,l-hexamethylpropyleneamine oxime (HMPAO) uptake and glutathione content in brain tumors. *J. Nucl. Med.* **1991**, *32*,

1675−1681. (c) Jacquier-Sarlin, M. R.; Polla, B. S.; Slosman, D. O. Oxido-reductive state: The major determinant for cellular retention of technetium-99m-HMPAO. *J. Nucl. Med*. **1996**, *37*, 1413−1416. (d) Sasaki, T.; Toyama, H.; Oda, K.; Ogihara-Umeda, I.; Nishigori, H.; Senda, M. Assessment of antioxidative ability in brain: Technetium-99m-*meso*-HMPAO as an imaging agent for glutathione localization. *J. Nucl. Med*. **1996**, *37*, 1698−1701. (e) Sasaki, T.; Senda, M. Technetium-99m-*meso*-HMPAO as a potential agent to image cerebral glutathione content. *J. Nucl. Med*. **1997**, *38*, 1125−1129. (f) Ballinger, J. R.; Reid, R. H.; Gulenchyn, K. Y. Technetium-99m HM-PAO stereoisomers: Differences in interaction with glutathione.

(6) Jacquier-Sarlin, M. R.; Polla, B. S.; Slosman, D. O. Cellular Basis of ECD brain retention. *J. Nucl. Med*. **1996**, *37*, 1694−1697.

(7) (a) Lassen, N. A.; Sperling, B. ^{99m}Tc-bicisate reliably images CBF in chronic brain diseases but fails to show reflow hyperemia in subacute stroke: Report of a multicenter trial of 105 cases comparing ^{133}Xe and ^{99m}Tc-bicisate (ECD, Neurolite) measured by SPECT on the same day. *J. Cereb. Blood Flow Metab*. **1994**, *14*, S44−S48. (b) Moretti, J. L.; Caglar, M.; Weinmann, P. Cerebral perfusion imaging tracers for SPECT: Which one to choose? *J. Nucl. Med*. **1995**, *36*, 359−363.

(8) (a) Pietzsch, H. J.; Spies, H.; Hoffmann, S.; Stach, J. Lipophilic technetium complexes-V. Synthesis and characterization of (3-thiapentane-1,5-dithiolato) (thiophenolato) oxotechnetium(V). *Inorg. Chim. Acta* **1989**, *161*, 15−16. (b) Pietzsch, H. J.; Spies, H.; Hoffmann, H.; Scheller, D. Lipophilic technetium complexes-VII. Neutral oxotechnetium(V) complexes of tridentate Schiff-bases containing monothiols as co-ligands. *Appl. Radiat. Isot*. **1990**, *41*, 185−188. (c) Spies, H.; Pietzsch, H. J.; Syhre, R.; Hoffmann, S. Lipophilic technetium complexes-VIII. Preparation and animal studies of oxotechnetium(V) complexes with tridentate/monodentate ligand coordination. *Isotopenpraxis* **1990**, *26*, 159−162.

(9) (a) Mastrostamatis, S.; Papadopoulos, M.; Chiotellis, E.; Hunt, F. C. Tripodal NS_3-donor ligands as new backbone for reduced technetium. *Eur. J. Nucl. Med*. **1990**, *16*, 109. (b) Mastrostamatis, S.; Papadopoulos, M. S.; Pirmettis, I. C.; Paschali, E.; et al. Tridentate ligands containing the SNS donor atom set as a novel backbone for the development of technetium brain imaging agents. *J. Med. Chem*. **1994**, *37*, 3212−3218. (c) Spyriounis, D. M.; Pelecanou, M.; Stassinopoulou, C. I.; Raptopoulou, C. P.; Terzis, A.; Chiotellis, E. Synthesis and characteriztion of oxotechnetium(V) complexes with aza-substituted 2,6-dimethyl-4-azaheptane-2,6-dithiol ligands and benzyl mercaptan as coligand. *Inorg. Chem*. **1995**, *34*, 1077−1082. (d) Pirmettis, I. C.; Papadopoulos, M. S.; Mastrostamatis, C. P.; Raptopoulou, C. P.; Terzis, A.; Chiotellis, E. Synthesis and characterization of oxotechnetium(V) mixed-ligand complexes containing a tridentate N-substituted bis(2-mercaptoethyl)amine and a monodentate thiol. *Inorg. Chem*. **1996**, *35*, 1685−1691. (e) Papadopoulos, M. S.; Pirmettis, I. C.; Pelecanou, M.; Raptopoulou, C. P.; Terzis, A.; Stassinopoulou, C. I.; Chiotellis, E. *Syn-Anti* isomerism in a mixed-ligand oxorhenium complex ReO[SN(R)S][S]. *Inorg. Chem*. **1996**, *35*, 7377−7383. (f) Pirmettis, I. C.; Papadopoulos, M. S.; Chiotellis, E. Novel ^{99m}Tc aminobisthiolato/monothiolato "3 + 1" mixed ligand complexes: Structure−activity relationships and preliminary in vivo validation as brain blood flow imaging agents. *J. Med. Chem*. **1997**, *40*, 2539−2546. (g) Papadopoulos, M.; Pirmettis, I.; Raptopoulou, C.; Chiotellis, E.; Friebe, M.; Berger, R.; Spies, H.; Johannsen, B. Synthesis, structure, lipophilicity and protonation behaviour of mixed ligand rhenium chelates functionalized by amine groups. *Appl. Radiat. Isot*. **1998**, *49*, 961−966. (h) Jaipetch, T.; Pirmettis, I.; Papadopoulos, M.; Nock, B.; Maina, T.; Raptopoulou, C. P.; Terzis, A.; Chiotellis, E. Synthesis and characterization of two novel TcO and ReO mixed ligand complexes (3+1 combination, SNS/S) for hypoxia imaging. *IAEA TEC-DOC-1029* **1998**, 231−242.

(10) (a) Nock, B.; Maina, T.; Pirmettis, I.; Papadopoulos, M.; Tsoukalas, C.; Chiotellis, E. The potential role of intracerebral glutathione in the retention of a representative ^{99m}Tc SNS/S mixed ligand complex in mice brain. *Czech. J. Phys*. **1998**, *48*, 75−80. (b) Nock, B.; Maina, T.; Pirmettis, I.; Papadopoulos, M.; Tsoukalas, C.; Chiotellis, E. Reaction with glutathione, a possible mechanism involved in rodent brain retention of a ^{99m}Tc SNS/S complex containing a pendant ester functionality. *IAEA TEC-DOC-1029* **1998**, 79−89. (c) Nock, B.; Tsoukalas, C.; Maina, T.; Pirmettis, I.; Papadopoulos, M.; Spies, H.; Johannsen, B.; Chiotellis, E. Comparative stability versus cysteine of mixed ligand ^{99m}Tc complexes containing monothiols of differing nucleophilicity. *Eur. J. Nucl. Med*. **1997**, *24*, 990. (d) Pelecanou, M.; Pirmettis, I. C.; Nock, B. A.; Papadopoulos, M.; Chiotellis, E.; Stassinopoulou, C. I. Interaction of glutathione with MO(SNS)(S) (M= Re, ^{99m}Tc) mixed ligand complexes. Isolation and characterization of the adduct. *Inorg. Chim. Acta* **1998**, *281*, 148−152.

(11) (a) Meister, A.; Anderson, M. E. Glutathione. *Annu. Rev. Biochem*. **1983**, *52*, 711−760. (b) Reichert, D. Toxication of foreign substances by conjugation reactions. *Angew. Chem*. **1981**, *20*, 135−216. (c) Griffith, O. W.; Meister, A. Glutathione: Interorgan translocation, turnover, and metabolism. *Proc. Natl. Acad. Sci. U.S.A*. **1979**, *76*, 5606−5610. (d) Plummer, J. L.; Smith, B. R.; Sies, H.; Bend, J. R. Chemical depletion of glutathione in vivo. *Methods Enzymol*. **1981**, *77*, 50−59.

(12) Papadopoulos, M.; Pirmettis, I.; Tsoukalas, C.; Nock, B.; Maina, T.; Raptopoulou, C. P.; Terzis, A.; Friebe, M.; Spies, H.; Johannsen, B.; Chiotellis, E. Study on the formation of mixed ligand oxorhenium and oxotechnetium complexes (SNS/S) combination. *IAEA TEC-DOC-1029* **1998**, 141−155.

(13) (a) Rabenstein, D. L. Nuclear magnetic resonance studies of the acid−base chemistry of amino acids and peptides. I. Microscopic ionization constants of glutathione and methylmercury-complexed glutathione. *J. Am. Chem. Soc*. **1973**, *95*, 2797−2803. (b) Backs, S. J.; Rabenstein, D. L. Nuclear magnetic resonance studies of the solution chemistry of metal complexes. 16. Complexation of trimethyllead by sulfydryl-containing amino acids and related molecules. *Inorg. Chem*. **1981**, *20*, 410−415.

(14) (a) March, J. The neighboring group mechanism. *Advanced Organic Chemistry*; John Wiley & Sons: New York, Toronto, Singapore, 1985; pp 268−272. (b) Deutsch, E.; Root, M. J.; Nosco, D. L. Mechanistic aspects of transition metal complexes containing coordinated sulphur. In *Advances in Inorganic and Bioinorganic Mechanisms*; Sykes, E. D., Ed.; Academic Press: London, 1982; Vol. 1, p 269. (c) Asher, L. E.; Deutsch, E. Effect of added ligands on the rate of chromium−sulfur bond fission in thiolatopentaaquochromium(III) complexes. Evidence for a sulfur-induced trans effect in chromium(III) chemistry. *Inorg. Chem*. **1976**, *15*, 1531−1537. (d) Asher, L. E.; Deutsch, E. Preparation and aquation kinetics of the pentaaquo(2-mercaptoethylammonium-*S*)chromium(III) ion. Origin of the k_o term in rate laws of the form $d(\ln[H_2O)_5CrX]^{n+})/dt = k_o + k_1(H^+)$. *Inorg. Chem*. **1973**, *12*, 1774−1778. (e) Asher, L. E.; Deutsch, E. Preparation and aquation kinetics of the pentaaquo(4-thioanilinium-*S*)chromium-(III) ion. Catalysis of chromium−sulfur bond breaking by oxygen and other oxidants. *Inorg. Chem*. **1972**, *11*, 2927−2933.

(15) (a) Ishikawa, T.; Li, Z. S.; Lu, Y. P.; Rea, P. A. The GS-X pump in plant, yeast, and animal cells: Structure, function, and gene expression. *Biosci. Rep*. **1997**, *17*, 189−207. (b) Shen, H.; Paul, S.; Breuninger, L. M.; Ciaccio, P. J.; Laing, N. M.; Helt, M.; Tew, K. D.; Kruh, G. D. Cellular and in vitro transport of glutathione conjugates by MRP. *Biochemistry* **1996**, *35*, 5719−5725. (c) Khanna, P.; Kumari, K.; Ansari, N. H.; Srivastava, S. K. ATP-dependent transport of glutathione-*N*-ethylmaleimide conjugate across erythrocyte membrane. *Biochem. Med. Metab. Biol*. **1994**, *53*, 105−114. (d) Scott, R. B.; Matin, S.; Hamilton, S. C. Glutathione, glutathione S-transferase, and transmembrane transport of glutathione conjugate in human neutrophil leukocytes. *J. Lab. Clin. Med*. **1990**, *116*, 674−680.

(16) (a) Griffith, O. W.; Meister, A. Translocation of intracellular glutathione to membrane-bound γ-glutamyl transpeptidase as a discrete step in the γ-glutamyl cycle: Glutathionuria after inhibition of transpeptidase. *Proc. Natl. Acad. Sci. U.S.A*. **1979**, *76*, 268−272. (b) Griffith, O. W.; Meister, A. Excretion of cysteine and γ-glutamyl-cysteine moieties in human and experimental animal γ-glutamyl transpeptidase deficiency. *Proc. Natl. Acad. Sci. U.S.A*. **1980**, *77*, 3384−3387. (c) Griffith, O. W.; Bridges, R. J.; Meister, A. Formation of γ-glutamylcyst(e)ine in vivo is catalyzed by γ-glutamyl transpeptidase. *Proc. Natl. Acad. Sci. U.S.A*. **1981**, *78*, 2777−2781.

(17) (a) Huang, J.; Philbert, M. A. Distribution of glutathione and glutathione-related enzyme systems in mitochondria and cytosol of cultured cerebellar astrocytes and granule cells. *Brain Res*. **1995**, *680*, 16−22. (b) Bellomo, G.; Palladini, G.; Vairetti, M. Intranuclear distribution, function and fate of glutathione and glutathione-S-conjugate in living rat hepatocytes studied by fluorescence microscopy. *Microsci. Res. Technol*. **1997**, *36*, 243−252. (c) Bellomo, G.; Vairetti, M.; Stivala, L.; Mirabelli, F.; Richelmi, P.; Orrenius, S. Demonstration of nuclear compartmentalization of glutathione in hepatocytes. *Proc. Natl. Acad. Sci. U.S.A*. **1992**, *89*, 4412−4416.

(18) (a) Yamazaki, M.; Suzuki, H.; Sugiyama, Y. Recent advances in carrier-mediated hepatic uptake and biliary excretion of xenobiotics. *Pharm. Res*. **1996**, *14*, 497−513. (b) Hinchman, C. A.; Ballatori, N. Glutathione conjugation and conversion to mercapturic acids can occur as an intrahepatic process. *J. Toxicol. Environ. Health* **1994**, *41*, 387−409. (c) Sekura, R.; Meister, A. Glutathione turnover in the kidney; considerations relating to the γ-glutamyl cycle and the transport of amino acids. *Proc. Natl. Acad. Sci. U.S.A*. **1974**, *71*, 2969−2972.

(19) Kannan, R.; Kuhlenkamp, J. F.; Jeandidier, E.; et al. Evidence for carrier-mediated transport of glutathione across the blood-brain barrier in the rat. *J. Clin. Invest*. **1990**, *85*, 2009−2013.

(20) (a) Marstein, S.; Jellum, E.; Nesbakken, R.; Perry, T. L. Biochemical investigations of biopsied brain tissue and autopsied organs from a patient with pyroglutamic acidemia (5-oxoprolinemia). *Clin. Chim. Acta* **1981**, *111*, 219−228. (b) Perry, T.; Yong, V. W. Idiopathic Parkinson's disease, progressive supra-

nuclear palsy and glutathione metabolism in the substantia nigra of patients. *Neurosci. Lett.* **1986**, *67*, 269−274. (c) Slivka, A.; Spina, M. B.; Cohen, G. Reduced and oxidized glutathione in human and monkey brain. *Neurosci. Lett.* **1987**, *74*, 112−118.

(21) (a) Babich, J. W. Technetium-99m-HMPAO retention and the role of glutathione: the debate continues (Editorial). *J. Nucl. Med.* **1991**, *32*, 1681−1683. (b) Bates, S. E.; Regis, J. I.; Robey, R. W.; Zhan, Z.; Scala, S.; Meadows, B. J. Chemoresistance in the clinic: overview 1994. *Bull. Cancer* **1994**, *81*, 55S−61S. (c) O'Brien, M. L.; Tew, K. D. Glutathione and related enzymes in multidrug resistance. *Eur. J. Cancer* **1996**, *32A*, 967−978. (d) Muller, M.; de Vries, E. G.; Jansen, P. L. Role of multidrug resistance protein (MRP) in glutathione S-conjugate transport in mammalian cells. *J. Hepatol.* **1996**, *24*, 100−108. (e) Zhang, K.; Wong, K. P. Active transport of glutathione S-conjugate in human colon adenocarcinoma cells. *Cancer Lett.* **1996**, *108*, 143−151. (f) Newkirk, K.; Heffern, J.; Slosman-Moll, E.; Sessions, R. B.; Rasmussen, A. A.; Andrews, P. A.; Cullen, K. J. Glutathione content but not glutamyl cysteine synthetase mRNA expression predicts cisplatin resistance in head and neck cancer cell lines. *Cancer Chemother. Pharmacol.* **1997**, *40*, 75−80. (g) Kabasakal, L.; Oezker, K.; Hayward, M.; Akansel, G.; Griffith, O.; et al. Technetium-99m sestamibi uptake in human breast carcinoma cell lines displaying glutathione-associated drug-resistance. *Eur. J. Nucl. Med.* **1996**, *23*, 568−570.

(22) (a) Johannsen, B.; Scheunemann, M.; Spies, H.; Brust, P.; Wober, J.; Syhre, R.; Pietzsch, H. J. Technetium(V) and rhenium(V) complexes for 5-HT_{2A} serotonin receptor binding: Structure-affinity considerations. *Nucl. Med. Biol.* **1996**, *23*, 429−438. (b) Johannsen, B.; Berger, R.; Brust, P.; Pietzsch, H. J.; Schenker, C.; Seifert, S.; Syhre, R.; Spies, H. Structural modifications of receptor-binding technetium-99m complexes in order to improve brain uptake. *Eur. J. Nucl. Med.* **1997**, *24*, 316−319. (c) Meegalla, S.; Ploessl, K.; Kung, M. P.; Chumpradit, S.; Stevenson, D. A.; Frederick, D.; Kung, H. F. Tc-99m-labeled tropanes as dopamine transporter imaging agents. *Bioconjugate Chem.* **1996**, *7*, 421−429. (d) Meegalla, S.; Ploessl, K.; Kung, M. P.; Stevenson, D. A.; Liable-Sands, L. M.; Rheingold, A. L.; Kung, H. F. First example of a ^{99m}Tc complex as a dopamine transporter imaging agent. *J. Am. Chem. Soc.* **1995**, *117*, 11037−11038.

(23) (a) Corbin, J. L.; Miller, K. F.; Rariyadath, N.; Wherland, S.; Bruce, L. A.; Stiefel, E. I. Preparation and properties of tripodal and linear tetradentate N,S-donor ligands and their complexes containing the MoO_2^{2+} core. *Inorg. Chim. Acta* **1984**, *90*, 41−51. (b) Mann, F. Hofman's ethylene bases. Synthesis of β,β'-diaminodiethylamine and β,β'-diaminodiethylmethylamine. *J. Chem. Soc.* **1934**, 461−466. (c) Harley-Mason, J. Some aliphatic thiols and their derivatives. Part I. Aliphatic mercaptans. *J. Chem. Soc.* **1947**, 320−322. (d) Wineman, R. J.; Gollis, M. H.; James, J. C.; Pomponi, A. M. Thioethylation of amines with ethylene sulfide. *J. Org. Chem.* **1962**, *27*, 4222−4226.

(24) Otto, C. A.; Brown, L. E.; Lee, H. Subcellular distribution of [^{125}I]-iodoaryl β-methyl fatty acids. *Int. J. Nucl. Med. Biol.* **1985**, *12*, 223−226.

JM980174F